$NaCH_2X$ when X = SiH_3, PH_2, and SH are quite obvious. The predicted stabilities of free anions decreases in the order X = SiH_3 > PH_2 > Cl > SH > F > OH > H > NH_2 > CH_3, while the order in the organolithium compounds, $LiCH_2X$, is X = Cl > F > SiH_3 > OH > SH > NH_2 > PH_2 > H > CH_3. The $NaCH_2X$ species have the same relative energies as the free anions for first-row X substituents; for the second-row groups, the order of stabilities is the same as that for $LiCH_2X$.

In solution, either the organometallics are aggregated or the metal is solvated. Nevertheless, both solution and X-ray crystallographic studies indicate that the metal is closely associated to the formal anionic center.[4] The stabilities of anionic species in solution should follow an order intermediate between those calculated for the free anions and for the organometallics, since the anion is never really free. The calculations on monomers overestimate the tightness of association of the metal cation to the anion.

Finally, we note the close parallel between the tendency of lithium to bridge in the α-first-row heteroatom-substituted carbanions and the bridged structures found by Del Bene et al.[20] when Li^+ cations associate with the isoelectronic neutral analogues, NH_2NH_2, NH_2OH, NH_2F, etc. For example, the conformation of hydrazine alters so that both lone pairs can interact simultaneously with Li in the $N_2H_4Li^+$ complex.

Acknowledgment. We are grateful to the Deutsche Forschungsgemeinschaft, the Fonds der Chemischen Industrie, the National Science Foundation, and the Alexander von Humboldt Foundation for support of this research, to the staff of the Regionales Rechenzentrum Erlangen for their cooperation, and to Professor Theodore Cohen for helpful comments.

Registry No. CH_4, 74-82-8; CH_3CH_3, 74-84-0; CH_3NH_2, 74-89-5; CH_3OH, 67-56-1; CH_3F, 593-53-3; CH_3SiH_3, 992-94-9; CH_3PH_2, 593-54-4; CH_3SH, 74-93-1; CH_3Cl, 74-87-3; $^-CH_3$, 15194-58-8; $^-CH_2CH_3$, 25013-41-6; $^-CH_2NH_2$, 74215-21-7; $^-CH_2OH$, 55830-71-2; $^-CH_2F$, 60291-31-8; $^-CH_2SiH_3$, 57271-97-3; $^-CH_2PH_2$, 84005-13-0; $^-CH_2SH$, 51422-57-2; $^-CH_2Cl$, 60291-29-4; $LiCH_3$, 917-54-4; $LiCH_2CH_3$, 811-49-4; $LiCH_2NH_2$, 59189-59-2; $LiCH_2OH$, 59189-60-5; $LiCH_2F$, 59189-61-6; $LiCH_2SiH_3$, 91230-25-0; $LiCH_2PH_2$, 91230-26-1; $LiCH_2SH$, 91230-27-2; $LiCH_2Cl$, 18645-12-0; $NaCH_3$, 18356-02-0; $NaCH_2CH_3$, 676-54-0; $NaCH_2NH_2$, 91230-28-3; $NaCH_2OH$, 91230-29-4; $NaCH_2F$, 91230-30-7; $NaCH_2SiH_3$, 91230-31-8; $NaCH_2PH_2$, 91230-32-9; $NaCH_2SH$, 91230-33-0; $NaCH_2Cl$, 91230-34-1; Li^+NH_3, 52472-72-7; Li^+OH_2, 35163-45-2; Li^+FH, 60790-38-7; Li^+PH_3, 61817-05-8; Li^+SH_2, 91230-36-3; Li^+ClH, 91230-37-4; Na^+NH_3, 57450-14-3; Na^+OH_2, 36606-66-3; Na^+FH, 60790-39-8; Na^+PH_3, 91230-39-6; Na^+SH_2, 91230-40-9; Na^+ClH, 91230-41-0.

Tricarbon Monoxide—A Theoretical Study

Ronald D. Brown* and E. H. N. Rice

Contribution from the Chemistry Department, Monash University,
Clayton, Victoria, Australia 3168. *Received August 22, 1983*

Abstract: On the basis of molecular orbital calculations at the HF level with 6-31G* basis and MP3 correlation correction, C_3O is predicted to be a stable linear molecule with a singlet ground state. The lowest triplet state lies 168 kJ mol^{-1} above this. The fully optimized geometry leads to a predicted rotational constant within 0.2% of that determined experimentally from the microwave spectrum. C_3O is predicted to be stable with respect to dissociation into C_2 + CO by 433 kJ mol^{-1} and to have $\Delta H_f°$ of 282 kJ mol^{-1}. The dipole moment is predicted to be 1.85 D compared with the experimental value of 2.391 D. Various possible dimers were studied at the HF/STO-3G level. We conclude that gas-phase dimerization of C_3O is not likely to be rapid. A preliminary study of the reaction pathway for $C_3O + C_2H_4$ implies that reaction will not be rapid. Both the predicted internuclear distances and the Mulliken population analysis imply that the CC bonds are double and the CO bond is of somewhat higher order. The description in terms of Pauling resonance structures seems to represent the structure quite well.

Theoretical studies of the oxides of carbon have been almost exclusively devoted to CO and CO_2 although there has been some consideration of the well-known higher homologue of CO_2—tricarbon dioxide (carbon suboxide, C_3O_2). For example, Pauling,[1a] in a discussion of CO_2 and related molecules, discussed the geometry of C_3O_2 and wrote down resonance structures that include $^-O{-}C{\equiv}C{-}C{\equiv}O^+$. His analogous discussion[1b] of CO did not, however, include speculation about possible higher homologues for which analogous resonance forms could be written, the simplest being tricarbon monoxide, C_3O, for which a polar resonance form $^-C{\equiv}C{-}O{\equiv}O^+$ can be written, analogous to $^-C{\equiv}O^+$ for carbon monoxide.

Quantum chemical calculations on the oxides of carbon have been focused on CO, CO_2, and the oxycumulenes, C_nO_2, especially C_3O_2. We have been unable to find any previous theoretical study of C_3O.

Table I. Structure and Geometrical Parameters for C_3O

$C_3{-}C_2{-}C_1{-}O$

	optimum bond lengths (pm) in C_3O		
level of calc/basis	C_3C_2	C_2C_1	CO
HF/STO-3G	125.6	129.2	116.9
HF/3-21G	125.7	127.9	114.7
HF/4-31G	126.0	128.1	114.7
HF/6-31G*	125.6	129.5	112.9
MP3/6-31G*	127.2	130.3	115.1

Since simple valency arguments suggest that C_3O might bear the same relation to CO as does C_3O_2 to CO_2, we have speculated on the possibility of it intervening in the galactochemistry of interstellar molecular clouds. An extension of our theoretical model of such clouds[2] indicated that C_3O might be detectable in some molecular clouds. Preliminary investigations predict an abundance of C_3O similar to that of HC_3N, a widely observed interstellar species. It also seemed possible that a laboratory detection might be feasible.[3] As a basis for planning the gen-

---

(1) Pauling, L. "The Nature of the Chemical Bond", 3rd ed.; Cornell University Press: Ithaca, NY, 1960; pp 267–269. (b) Reference 1a, pp 265–267.

(2) Brown, R. D.; Rice, E. *Philos. Trans. R. Soc. London, Ser. A*, **1981**, *303*, 523–533.

0002-7863/84/1506-6475$01.50/0

Table II. Vibrational Frequencies (cm^{-1}) for C_3O (HF/3-21G//HF/3-21G)

	3-21G	cor^a
π	230	200
π	810	720
σ	1140	1010
σ	2120	1890
σ	2470	2200

^{a}Correction factor of 0.89 applied to 3-21G results as suggested by Pople et al.[16]

eration and detection via microwave spectroscopy, we accordingly embarked on an ab initio molecular orbital study of C_3O which we report in the present paper. It is gratifying that our results have already led to the spectroscopic characterization of C_3O.[4]

Theoretical Methods

In this study calculations were performed by using the GAUSSIAN 80 system of programs.[5] Electron correlation was included by using Moller-Plesset perturbation theory carried to second (MP2) and third (MP3) order[6] with the core molecular orbitals frozen.[7] For calculations at the Hartree-Fock level (HF), minima in the potential surface were located by using analytical gradient methods. At the MP3 level the minima were located by using parabolic interpolation.

Several basis sets were used in this work: the minimal STO-3G basis set,[8] the split-valence 3-21G[9] and 4-31G[10] basis sets, the double-ζ (DZ) basis set of Dunning and Hay,[11] and the 6-31G* basis set[12] which includes d-polarization functions on heavy atoms.

Results and Discussion

Equilibrium Structure of C_3O. A linear structure for C_3O was found at both the HF and MP3 levels (Table I). At an STO-3G level we expect bonds to oxygen atoms to be too long when compared with experimentally obtained values and CC bonds to be short by 2–3 pm.[13] With a 4-31G basis set, CC bonds are usually still too short, but CO bonds are in reasonable agreement (to within ~1 pm) with experiment.[13] HF/6-31G* studies of compounds containing CC and CO bonds[14] indicate that bond lengths are predicted to be ~2 pm short at that level. The same study shows that CC and CO bond lengths at the MP3/6-31G* level deviate by ~0.5 pm from experimental values. The results shown in Table I seem consistent with these general trends given that the MP3 results are close to the experimental values.

Table III. CO Stretch Frequencies (cm^{-1})

molecule	frequency
CO	2170^a
CO_2	2349^b
C_3O_2	2258^b
H_2CCO	2152^b
H_2CCCO	2100^c

^{a}Reference 17. ^{b}Reference 18. ^{c}Reference 19.

Table IV. MP3/6-31G* Rotational Constants for C_3O (MHz)

isotopic species	B_e	B_0(estim)	B_0(obsd)[4]
$^{12}C^{12}C^{12}C^{16}O$	4771	4814^a	4810.9
$^{13}C^{12}C^{12}C^{16}O$	4595	4633^b	
$^{12}C^{13}C^{12}C^{16}O$	4746	4786^b	
$^{12}C^{12}C^{13}C^{16}O$	4758	4798^b	
$^{12}C^{12}C^{12}C^{18}O$	4535	4573^b	

^{a}Scaled by using B_0(exptl)/B_e(theory) for HC_3N, viz. 1.0091, at MP3/6-31G* level. ^{b}Scaled by using B_0(exptl)/B_e(theory) for $^{12}C^{12}C^{12}C^{16}O$ (=1.0084) at MP3/6-31G* level.

Table V. MP3/6-31G* Equilibrium Geometry for HC_3N (pm)

	calcd	r_s[21]
C_3H	106.8	105.7
C_3C_2	120.7	120.5
C_2C_1	138.8	137.8
C_1N	116.3	115.9

Table VI. MP3/6-31G* Rotational Constants for HC_3N (MHz)

isotopic species	B_e	B(obsd)[22]
$H^{12}C^{12}C^{12}C^{14}N$	4508	4549.05896 (14)
$D^{12}C^{12}C^{12}C^{14}N$	4183	4221.58167 (44)
$H^{13}C^{12}C^{12}C^{14}N$	4369	4408.4423 (11)
$H^{12}C^{13}C^{12}C^{14}N$	4489	4529.7617 (13)
$H^{12}C^{12}C^{13}C^{14}N$	4490	4530.19760 (46)
$H^{12}C^{12}C^{12}C^{15}N$	4377	4416.75278 (98)

The predicted bond lengths (MP3) imply that all bonds have a bond order greater than two, both CC bonds being shorter than that of ethylene (134 pm) and the CO bond length being between that of formaldehyde (121 pm) and carbon monoxide (113 pm). Simplistically, we might view the CO bond in much the way discussed by Pauling for CO and CO_2 which would be in line with regarding C_3O as describable by structures such as

$$\underset{\text{I}}{{}^{-}C{\equiv}C{-}C{\equiv}O^{+}} \qquad \underset{\text{II}}{:C{=}C{=}C{=}\ddot{O}:}$$

$$\underset{\text{III}}{:C{=}C{=}C{=}\underset{\cdot\cdot}{O}:} \qquad \underset{\text{IV}}{{}^{+}:C{-}C{\equiv}C{-}O:^{-}}$$

From these one might also infer that the CC bonds should be slightly shorter than an ethene bond (cf. Pauling's discussion as to why the CO bonds of CO_2 are shorter than the "standard" double bond length[1a]).

A Mulliken population analysis[15] at the HF/STO-3G level yields an overlap population between C_3 and C_2 of 0.64 e which is slightly larger than that obtained for ethene (0.61 e). The C_2–C_1 overlap population is 0.58 e, slightly less than the ethene value. The C_1–O overlap population of 0.51 e is very close to the C–O overlap in CO (0.52 e) and somewhat larger than that obtained for H_2CO (0.45 e) and CO_2 (0.45 e). This is in keeping with the CO bond being stronger than a double bond. The CC bonds, however, are close to typical double bond values with the C_3C_2 bond being stronger than the C_2C_1 bond.

Vibrational Analysis. The harmonic vibrational frequencies of C_3O have been determined at an HF/3-21G level for the HF/3-21G equilibrium geometry. A study of 486 frequencies from 38 species by Pople et al.[16] at the HF/3-21G level suggests that 3-21G frequencies should be scaled by 0.89 to predict experimental frequencies. The calculated frequencies for C_3O and the scaled frequencies are presented in Table II.

---

(3) The generation of C_3O by reaction of C atoms with CO in an Ar matrix has been claimed by DeKock and Weltner, on the basis of an infrared band at 2241 cm^{-1}. DeKock, R. L.; Weltner, W. *J. Am. Chem. Soc.* **1971**, *93*, 7106–7107. No further support of this claim appears to have been forthcoming.

(4) Brown, R. D.; Eastwood, F. W.; Elmes, P.; Godfrey, P. D. *J. Am. Chem. Soc.* **1983**, *105*, 6496–6497.

(5) Binkley, J. S.; Whiteside, R. A.; Krishnan, R.; Seeger, R.; DeFrees, D. J.; Schlegal, H. B.; Topiol, S.; Kahn, L. R.; Pople, J. A. *QCPE* **1981**, *13*, 406.

(6) Pople, J. A.; Binkley, J. S.; Seeger, R. *Int. J. Quantum Chem. Symp.* **1976**, *10*, 1–19.

(7) DeFrees, D. J.; Levi, B. A.; Pollack, S. K.; Hehre, W. J.; Binkley, J. S.; Pople, J. A. *J. Am. Chem. Soc.* **1979**, *101*, 4085–4089.

(8) Hehre, W. J.; Stewart, R. F.; Pople, J. A. *J. Chem. Phys.* **1969**, *51*, 2657–2664.

(9) Binkley, J. S.; Pople, J. A.; Hehre, W. J. *J. Am. Chem. Soc.* **1980**, *102*, 939–947.

(10) Ditchfield, R.; Hehre, W. J.; Pople, J. A. *J. Chem. Phys.* **1971**, *54*, 724–728.

(11) Dunning, T. H.; Hay, P. J. In "Methods of Electronic Structure Theory"; Schaefer, H. F., Ed.; Plenum Press: NY, 1977; pp 1–27.

(12) Hariharan, P. C.; Pople, J. A. *Theor. Chim. Acta* **1973**, *28*, 213–222.

(13) Pople, J. A. In "Applications of Electronic Structure Theory"; Schaefer, H. F. III, Ed.; Plenum Press: NY, 1977; pp 1–27.

(14) DeFrees, D. J. Raghavachari, K.; Schlegel, H. B.; Pople, J. A. *J. Am. Chem. Soc.* **1982**, *104*, 5576–5580.

(15) Mulliken, R. S. *J. Chem. Phys.* **1955**, *23*, 1833–1840.

(16) Pople, J. A.; Schlegel, H. B.; Krishnan, R.; DeFrees, D. J.; Binkley, J. S.; Frisch, M. J.; Whiteside, R. A.; Hout, R. F.; Hehre, W. J. *Int. J. . Quantum Chem. Symp.* **1981**, *15*, 269–278.

Table VII. Energetics of the C_3O System (in hartrees)

molecule	E(MP3/6-31G*)	zero-point motion correction
C_3O	−188.8501	1.56×10^{-2}
C_2	−75.6606	4.94×10^{-3}
CO	−113.0185	4.23×10^{-3}

Table VIII. Dipole Moment (D)

molecule	4-31G[a]	6-31G*[a]	exptl/D
C_3O	1.10[b]	1.85[b]	2.391[d]
CO	0.60[c]	0.26[c]	0.112[b,e]

[a] Calculated at equilibrium geometry for basis set. [b] Positive end of dipole is at oxygen end of molecule. [c] Positive end of dipole is at carbon end of molecule. [d] Reference 4. [e] Reference 26.

The frequency of 2241 cm^{-1} observed by DeKock and Weltner[3] and attributed by them to C_3O is in reasonable agreement with the scaled frequency of 2200 cm^{-1}. The experimental frequency is consistent with a molecule containing a CO structural feature similar to that present in carbon dioxide or carbon monoxide rather than more common organic carbonyl groupings but cannot yet be unambiguously ascribed to C_3O (see Table III for CO stretch frequencies of some related compounds).

Rotational Constant. Rotational constants computed from the MP3/6-31G* geometry are presented in Table IV for a number of isotopic forms of C_3O. DeFrees et al.[20] suggest that the accuracy of the predicted rotational constant can be improved by applying a scaling to the theoretical constants, where the scaling factor is obtained by averaging B_0(exptl)/B_e(theory) over a number of molecules structurally similar to the unknown system. HC_3N is isoelectronic with C_3O and also linear. Table V contains the structural parameters for HC_3N at the MP3/6-31G* level. Included in Table V are the r_s parameters of Costain[21] for comparative purposes. The predicted rotational constants and the experimentally determined constants for a number of isotopic species are displayed in Table VI. From these values, B_0(exptl)/B_e(theory) was determined to be 1.0091. The scaled value of B_0 for the main isotope species of C_3O is presented in Table IV.

Subsequent to this prediction, an experimental value of B_0 for C_3O has been obtained by Brown et al.[4] via microwave spectroscopy. The estimated value is in very good agreement with the measured value, the difference being less than 0.2%. With HC_3N the value of B_0(exptl)/B_e(theory) for the different isotopic species varies by only 0.02%. Hence, using the experimental value of B_0 for C_3O we should be able to predict the B_0 values for other isotopic species to within 0.02% also. These values are listed as B_0(estim) in Table IV. Haese and Woods[23] have previously noted that the rotational transition frequencies of isotopic species can be precisely determined from a high-quality theoretical geometry and a known isotope's transition frequency.

Stability of C_3O. To determine whether C_3O is thermodynamically stable, we have calculated the energies of C_2 and CO in their singlet ground states at the MP3/6-31G* level (Table VII). The zero-point energy correction for C_3O was determined from the HF/3-21G vibrational frequencies, while the corrections for C_2 and CO were determined from the vibrational frequencies for the $^1\Sigma_g^+$ C_2 and $^1\Sigma^+$ CO states listed by Mizushima.[24]

Table IX. HF/6-31G Geometries for C_4O_2 (pm)

	$^1\Sigma_g^+$ C_4O_2	$^3\Sigma_g^-$ C_4O_2
C_1O_1	117.4	117.7
C_2C_1	127.2	127.1
C_3C_2	127.5	127.2

Table X. Energetics of the C_4O_2 System (hartrees)

	HF/6-31G	MP2/6-31G//HF/6-31G
CO	−112.66722	−112.87760
C_3O	−188.23618	−188.61531
singlet C_4O_2	−300.88855	−301.49340
triplet C_4O_2	−300.92125	−301.49614

From these values we see that C_3O is more stable than C_2 + CO by 449 or 433 kJ mol^{-1} after correction for zero-point motion. Using $\Delta H_f°$ (C2) = 829.3 kJ mol^{-1} and $\Delta H_f°$ (CO) = −113.8 kJ mol^{-1} [25] we estimate $\Delta H_f°$ (C_3O) to be 282 kJ mol^{-1}.

At the HF/6-31G* level the lowest triplet state is 168 kJ mol^{-1} above the singlet state (without zero-point motion correction). This indicates that the singlet state of C_3O is the ground state in agreement with the microwave results.[4]

Dipole Moment. The experimental and calculated dipole moments for C_3O and CO are presented on Table VIII. The inclusion of polarization functions leads to a significant improvement in the calculated dipole moments for both species. In the case of CO the measured dipole moment is in the opposite sense to that determined at the HF level.

Green,[27] in a study of dipole moments using configuration interaction (CI) with single and double excitations, obtains a value for the dipole moment of CO (0.088 D) close to the experimental value with the correct sense. The difference between the HF and CI dipole moment values is attributed to the $1\pi \rightarrow 2\pi$ polarizing excitation which transfers charge to the carbon. This is qualitatively the same as including the effects of a $^-C{\equiv}O^+$ resonance structure. The analogous resonance structure for C_3O, $^-C{\equiv}C{-}C{\equiv}O^+$, would lead to an increase in the dipole moment of C_3O.

Investigation of a Possible Formation Pathway: Dissociation of C_4O_2. When the possible routes to C_3O by pyrolysis of the compound $C_{12}H_{12}O_8$ were first considered,[4] it was thought that the pyrolysis might first yield C_4O_2 and that the production of C_3O might involve a subsequent fragmentation of C_4O_2 into C_3O and CO. It therefore seemed appropriate to study the energetics of this pathway. Lindner et al.[28] used semiempirical methods to investigate the stability of the oxycumulenes (O–C_n–O, n = 1–5). They found that oxycumulenes with an even number of carbon atoms have triplet ground states. Beebe and Sabin[29] performed MO-SCF calculations on C_2O_2 confirming that the $^3\Sigma_g^-$ stage of C_2O_2 is the lowest state. They also found the $^1\Sigma_g^+$ state to be bound. Haddon et al.,[30] using SCF and CI techniques with STO-3G and 4-31G basis sets, calculated that $^1\Sigma_g^+$ C_2O_2 was thermodynamically unstable with respect to two CO molecules and that there is a large barrier to dissociation via a $D_{\infty h}$ C–C stretch. However, for dissociation via trans bending, there is at most a small (~20 kJ mol^{-1}) barrier to dissociation.

We have determined the equilibrium geometries of $^1\Sigma_g^+$ and $^3\Sigma_g^-$ C_4O_2 at the HF/6-31G level (Table IX). The $^3\Sigma_g^-$ state was found to be lower in energy than the $^1\Sigma_g^+$ state by 86 kJ mol^{-1} in qualitative agreement with Lindner et al.[28] At this level the singlet C_4O_2 is thermodynamically unstable with respect to C_3O + CO by 39 kJ mol^{-1}. When MP2/6-31G is used at the HF/6-31G equilibrium geometries, the triplet–singlet separation is

---

(17) Herzberg, G. "Molecular Spectra and Molecular Structure"; Van Nostrand: Princeton, NJ, 1950; Vol. I, p. 522.

(18) Herzberg, G. "Molecular Spectra and Molecular Structure"; Van Nostrand: Princeton, NJ, 1967; Vol. III; pp 597–626.

(19) Brown, R. F. C.; Eastwood, F. W.; McMullen, G. L. *J. Am. Chem. Soc.* **1976**, *98*, 7421–7422.

(20) DeFrees, D. J.; Loew, G. H.; McLean, A. D. *Ap. J.* **1982**, *254*, 405–411.

(21) Costain, C. C. *J. Chem. Phys.* **1958**, *29*, 864–874.

(22) Lafferty, W. J.; Lovas, F. J. *J. Phys. Chem. Ref. Data* **1978**, *7*, 441–493.

(23) Haese, N. N.; Woods, R. C. *J. Chem. Phys.* **1980**, *73*, 4521–4527.

(24) Mizushima, M. "The Theory of Rotating Diatomic Molecules"; *Wiley*: NY, 1975; pp 403–409.

(25) Rosenstock, H. M.; Draxl, K.; Steiner, B. W.; Herron, J. T. *J. Phys. Chem. Ref. Data* **1977**, *6*, Suppl. 1.

(26) Rosenblum, B.; Nethercot, A. H.; Townes, C. H. *Phys. Rev.* **1958**, *109*, 400–412.

(27) Green, S. *J. Chem. Phys.* **1971**, *54*, 827–832.

(28) Lindner, P.; Öhrn, Y.; Sabin, J. R. *Int. J. Quantum Chem. Symp.* **1973**, *7*, 261–267.

(29) Beebe, N. H. F.; Sabin, J. R. *Chem. Phys. Lett.* **1974**, *24*, 389–394.

(30) Haddon, R. C.; Poppinger, D.; Radom, L. *J. Am. Chem. Soc.* **1975**, *97*, 1645–1649.

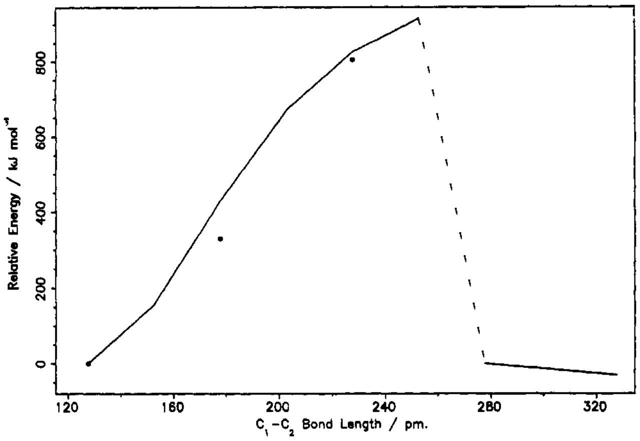

Figure 1. Relative energy vs. C_1C_2 bond length in C_4O_2. The data points indicate the MP2 results. Energies are relative to equilibrium C_4O_2.

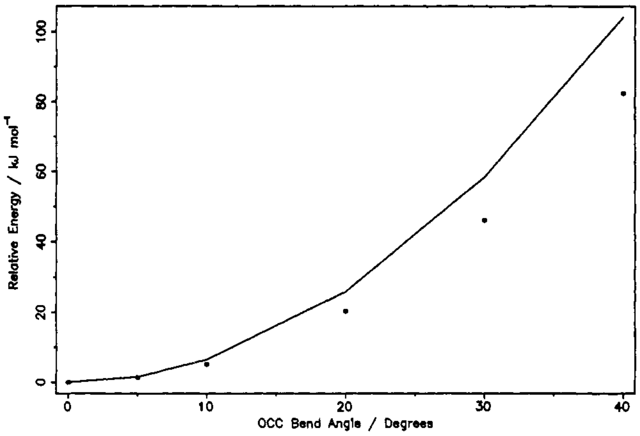

Figure 2. Relative energy vs. OCC bending angle in C_4O_2. The data points indicate the MP2 results. Energies are relative to equilibrium C_4O_2.

reduced to 7 kJ mol^{-1} and singlet C_4O_2 becomes more stable than C_3O + CO by 1 kJ mol^{-1}. The energy data are summarized in Table X.

To test for barriers to the dissociation of singlet C_4O_2 we have performed calculations at the HF/DZ level for various values of the bond length C_1C_2 and the angle OCC. For each calculation all geometrical parameters other than $r(C_1C_2)$ or OCC were varied to obtain a minimum energy structure. The results are presented in Figures 1 and 2. MP2/DZ calculations were performed at some of the HF/DZ geometries. These are also shown in Figures 1 and 2. The energies in these figures are relative to the $^1\Sigma_g{}^+$ C_4O_2 equilibrium energy. For both pathways there are considerable barriers to dissociation to C_3O and CO. This is the case for both the HF and MP2 calculations. Hence, we find $^1\Sigma_g{}^+$ C_4O_2 to be bound at both the HF and MP2 levels. The size of the barriers implies that if C_4O_2 is produced in its lowest singlet state it will not readily decompose into C_3O and CO. This is quite different to the behavior of $^1\Sigma_g{}^+$ C_2O_2 predicted by Haddon et al.

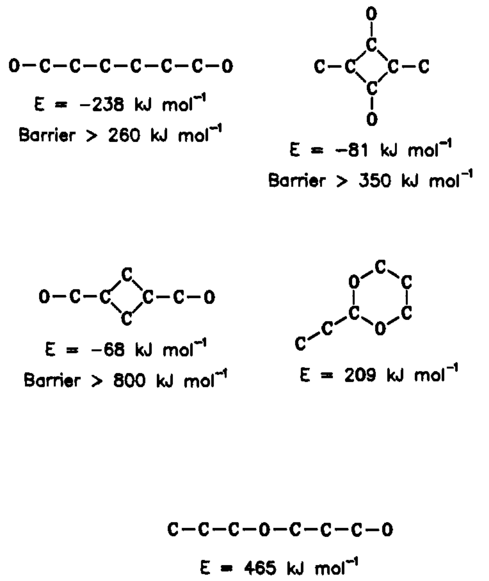

Figure 3. Dimers of C_3O. Energies are relative to two separated C_3O molecules.

Dimers of C_3O. To test the possibility of gas-phase dimerization of C_3O, we have computed the HF/STO-3G energies of a number of C_3O dimer structures. The energies and structures are shown in Figure 3. The energies shown are relative to two infinitely separated C_3O molecules. For the systems having energies lower than two C_3O molecules a barrier to combination has been assessed.

In all cases either the dimer is not energetically favorable or there is a large barrier to combination. This suggests that gas-phase dimerization is unlikely. These results should be treated with some caution due to the use of minimal basis sets, only a HF treatment, and the incomplete search of the potential surface.

We have also made a preliminary study of the reaction of C_3O with ethene. Exploratory calculations indicate that the optimum pathway to reaction involves an unsymmetrical arrangement of reactants and substantial kinking of the C_3O. An appreciable activation energy is involved, implying that C_3O will not be highly reactive toward ethene in the gas phase.

Registry No. C_3O, 11127-17-6; C_2H_4, 74-85-1.